–Supplementary Information–

Particle Morphology and Lithium Segregation to Surfaces of the $Li_7La_3Zr_2O_{12}$ Solid Electrolyte

Pieremanuele Canepa,[*,†] James A. Dawson,[†] Gopalakrishnan Sai Gautam,[‡] Joel M. Statham,[†] Stephen C. Parker,[†] and M. Saiful Islam[†]

†*Department of Chemistry, University of Bath, Bath, BA2 7AY, UK*

‡*Department of Mechanical and Aerospace Engineering, Princeton University, Princeton, NJ 08544, USA*

E-mail: P.canepa@bath.ac.uk

S1 Details of first-principles calculations

In order to develop the thermodynamic framework required to study bulk $Li_7La_3Zr_2O_{12}$ and its surfaces, first-principles calculations based on DFT are utilised. Here, DFT calculations rely on the generalized gradient approximation[1] within the projector-augmented wave framework as implemented in the Vienna Ab-Initio Simulation Package.[2–4] A wavefunction plane-wave cutoff of 520 eV together with Γ-centred k-point meshes with densities of 500 points per atoms were used to integrate the Brillouin-zone. With these settings, DFT energies and atomic forces were converged to within 0.05 meV per atom and 10^{-2} meV Å^{-1}, respectively. A well converged vacuum of 20 Å separated the slab from its replica along the non-periodic axis. While our surface models are all dipole free and charge neutral, the dipole correction was introduced to facilitate the convergence of the total energy.

S2 Chemical potentials bounds

To define the chemical potentials of the elements in $Li_7La_3Zr_2O_{12}$ in various tetrahedrons of the quaternary La-Li-Zr-O phase diagram one needs to solve simultaneously four equations relating the DFT total energies with the four chemical potentials, μ_{La}, μ_{Li}, μ_{Zr} and μ_{O}, respectively.

For example, the tetrahedron with vertices $Li_7La_3Zr_2O_{12}$, Li_2O, La_2O_3 and Zr is described by the following equations.

$$\begin{cases} E(\mathrm{Li_7La_3Zr_2O_{12}}) = 7\mu_{\mathrm{Li}} + 3\mu_{\mathrm{La}} + 2\mu_{\mathrm{Zr}} + 12\mu_{\mathrm{O}} \\ E(\mathrm{Li_2O}) = 2\mu_{\mathrm{Li}} + \mu_{\mathrm{O}} \\ E(\mathrm{La_2O_3}) = 2\mu_{\mathrm{La}} + 3\mu_{\mathrm{O}} \\ E(\mathrm{Zr}) = \mu_{\mathrm{Zr}} \end{cases}$$

where $E(\mathrm{Li_7La_3Zr_2O_{12}})$, $E(\mathrm{Li_2O})$, $E(\mathrm{La_2O_3})$ and $E(\mathrm{Zr})$ are the DFT total energies, respectively.

Table S1 show the bounds of chemical potentials derived from Figure 1 in the manuscript, and used in determining the surface energies of non-stoichiometric surfaces.

Table S1: Chemical potentials bounds La, Li, Zr and O in eV.

species	μ_{max}	μ_{min}
La	–5.487	–14.662
Li	–1.957	–5.016
Zr	–8.578	–20.812
O	–4.936	–11.052

S3 Surface energies

Table S2 and Figure S1 show the lowest surface energies γ of stoichiometric and non-stoichiometric $Li_7La_3Zr_2O_{12}$ surfaces. The structures of the surfaces of the $Li_7La_3Zr_2O_{12}$ matching the surface energies in Table S2 is attached to the manuscript.

Table S2: Surface energy γ (J m^{-2}) of La (blue), Li (red), O (green) and Zr (yellow) -terminated $Li_7La_3Zr_2O_{12}$ surfaces. Surface energies of non-stoichiometric slabs are derived using the chemical potentials from Table S1 and Figure 1 in the manuscript.

	Stoichiometric			non-stoichiometric		
	Zr	La	Li	La	Li	O
(010)	1.77	—	—	0.98	0.87±0.02	0.98
(001)	1.77	—	—	0.98	—	—
(101)	—	0.94	—	—	—	—
(011)	—	0.94	—	—	—	—
(110)	1.52	0.94	—	—	0.91	0.99
(111)	—	—	1.10	—	—	—
(021)	2.64	—	—	—	2.06	—

The non-stoichiometric surfaces in Figure S1 and Table S2 are the product of ordering procedures, where layers of Zr and/or La are selectively removed and charge-compensated by O removal. This requires the investigation of several number of atomic orderings (mostly orderings of Oxygen atoms). This task is simplified by computing with DFT only the 20 ordering arrangements with the lowest electrostatic energy, approximated by the Ewald energy computed from formal charges, i.e. Li = +1, La = +3, Zr = +4 and O = −2. From Figure S1 and Table S2 no number yet we note that several surface energies are identical for crystallographic planes symmetrically different in a typical tetragonal structure with space group ($I4_1/acd$). For example, the γ computed for the La-terminated stoichiometric (101) surface is equivalent to the surface energies obtained for (011) and (110) cuts, indicating the low degree of tetragonal distortion of the high-temperature cubic structure of $Li_7La_3Zr_2O_{12}$ $Ia3\bar{d}$. Similar conclusions can we drawn by surface energies of stoichiometric Zr-

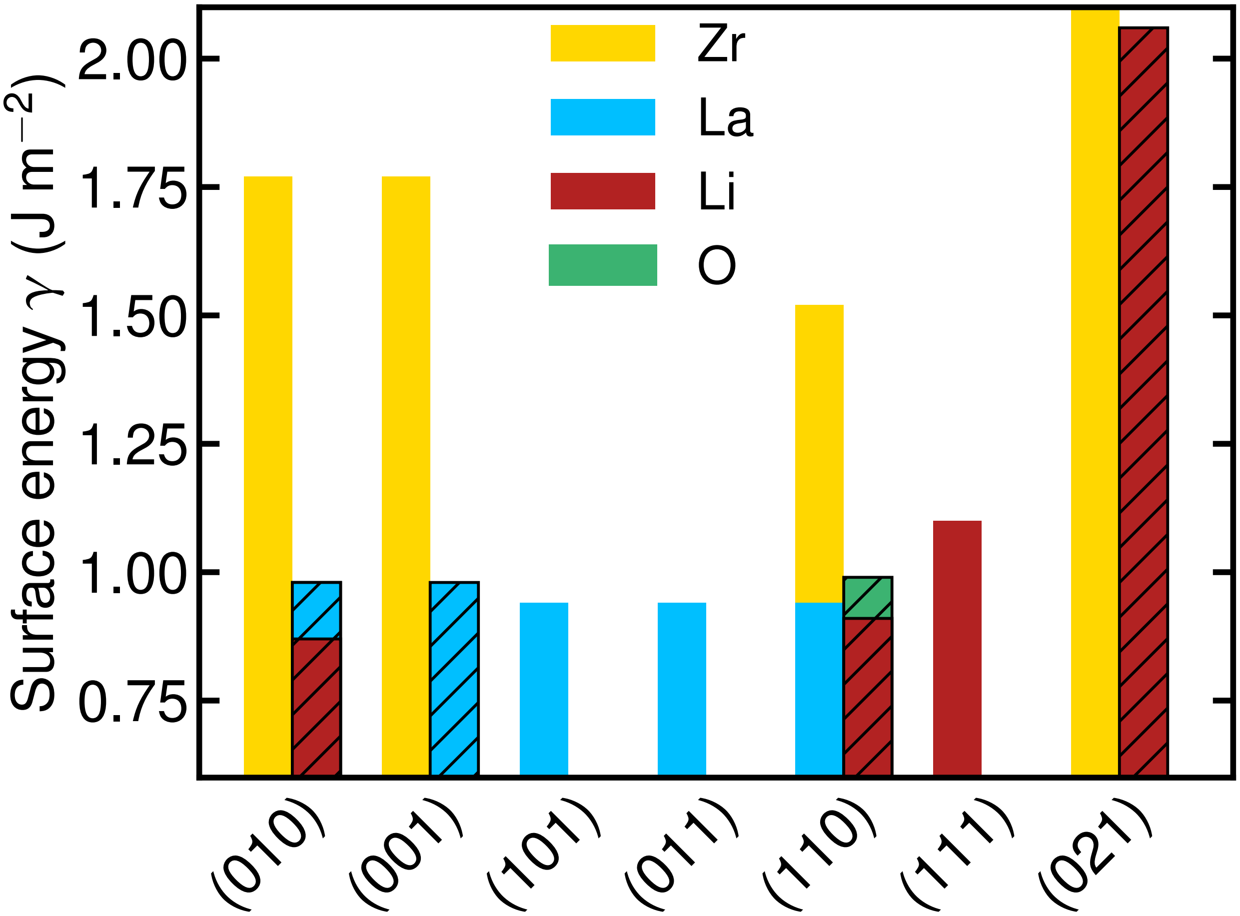

Figure S1: Surface energies γ (J m^{-2}) of La (blue), Li (red), O (green) and Zr (yellow) -terminated surfaces of $Li_7La_3Zr_2O_{12}$. Hatched bars indicate non-stoichiometric slabs, whose surface energies are derived using the chemical potentials from Figure 1b of the main manuscript.

terminated (010) and (001) surfaces, or the non-stoichiometric La-terminated (010) and (001) surfaces.

S4 $Li_7La_3Zr_2O_{12}$ particle morphologies

Figure S2 shows the particle equilibrium morphology of $Li_7La_3Zr_2O_{12}$ as function of temperature, including the 0 K (–273 °C) particle shape.

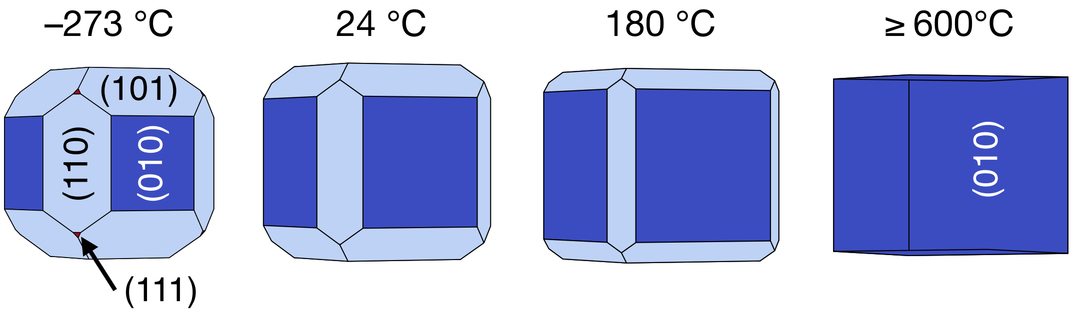

Figure S2: Computed equilibrium morphology of $Li_7La_3Zr_2O_{12}$ at various temperatures.

S5 $Li_7La_3Zr_2O_{12}$ surface reconstruction

Figure S3 shows the atomic arrangement of the La/O-terminated (011) surface of $Li_7La_3Zr_2O_{12}$, highlighting the coexistence of La and O layers, respectively. .

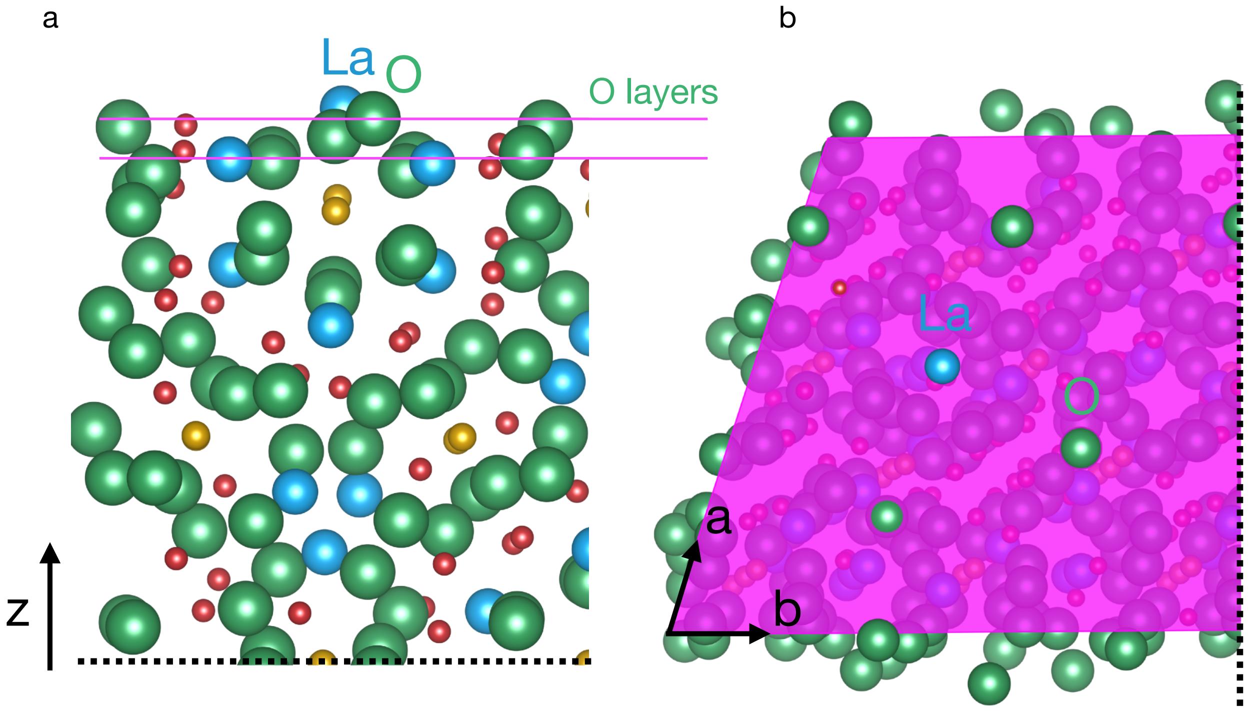

Figure S3: (**a**) Side-view and (**b**) top-view representation of the non-stoichiometric (011) La/O-terminated surface of $Li_7La_3Zr_2O_{12}$. Li atoms are in red, O in green, La in blue and Zr in gold. Solid lines identify the surface planes, highlighting the coexistence of planes of La and O atoms.

References

(1) Perdew, J. P.; Burke, K.; Ernzerhof, M. Generalized Gradient Approximation Made Simple. *Phys. Rev. Lett.* **1996**, *77*, 3865–3868.

(2) Kresse, G.; Joubert, D. From ultrasoft pseudopotentials to the projector augmented-wave method. *Phys. Rev. B* **1999**, *59*, 1758–1775.

(3) Kresse, G.; Furthmüller, J. Efficient iterative schemes for ab initio total-energy calculations using a plane-wave basis set. *Phys. Rev. B* **1996**, *54*, 11169–11186.

(4) Kresse, G.; Hafner, J. Ab initio molecular dynamics for liquid metals. *Phys. Rev. B* **1993**, *47*, 558–561.